FUSION OF LIDAR DATA AND OPTICAL IMAGERY FOR BUILDING MODELING

Liang-Chien Chen *, Tee-Ann Teo, Yi-Chen Shao, Yen-Chung Lai, Jiann-Yeou Rau

Center for Space and Remote Sensing Research, National Central University, Chung-Li, Taiwan.
(lcchen, ann, ycshao, stzac, jyrau)@csrsr.ncu.edu.tw

Commission WG IV/7

ABSTRACT:

This paper presents a scheme for building detection and building reconstruction from LIDAR data and optical imagery. The proposed scheme comprises two major parts: (1) detection of building regions, and (2) reconstruction of building models. Spatial registration of LIDAR data and optical images is performed as data preprocessing. Then, at the first stage, a region-based segmentation and knowledge-based classification are integrated to detect building regions. Once the building regions are detected, we analyze the coplanarity of the LIDAR raw data to shape the roof. The accurate position of walls of the building is determined by the integration of the edges extracted from optical imagery. Thus the three dimensional building edges can be used for the reconstruction. A patented method SMS (Split-Merge-Shape) is employed to generated building models in the last step. Having the advantages of high reliability and flexibility, the SMS method provides stable reconstruction even when those 3D building lines are broken. LIDAR data acquired by Leica ALS 40, QuickBird multispectral satellite images and aerial images were used in the validation.

1. INTRODUCTION

Building modeling is an essential task in the establishment of cyber city for city planning, management, and various applications. Building reconstruction may be performed by a photogrammetric procedure using aerial stereopairs. A number of researches have shown the approaches of combine data for building modeling, e.g., LIDAR (LIght Detecting And Ranging) and aerial image (Rottensteiner and Jansa, 2002), LIDAR and three-line-scanner image (Nakagawa, *et. al.*, 2002), LIDAR and high satellite image (Guo, 2003), LIDAR, aerial image and 2D map (Vosselman, 2002).

To improve the degree of automation, we propose here a scheme that integrates LIDAR data and optical images for building modeling. LIDAR data provide high accurate 3D points but lack breaklines information. On the contrary, optical imagery with high spatial resolution provides more accurate breaklines information than LIDAR data. Moreover, multispectral imagery is beneficial to identification and classification of objects, such as building and vegetation. Thus, we propose to combine LIDAR data and optical imagery, such as QuickBird multispectral satellite images and high spatial resolution aerial images, for the building modeling. The multispectral satellite images provide spectral information for detecting the building region, and the aerial images provide texture information for building reconstruction.

The proposed scheme comprises two major parts: (1) building detection, and (2) building reconstruction. Spatial registration of LIDAR data and optical imagery is performed as data preprocessing. The transformation between LIDAR space and image space is determined before the data fusion. It is done in such a way that two data sets are unified in the object coordinate system. Meanwhile, the exterior orientation

parameters of the optical imagery are recovered by employing ground control points. In the stage of building detection, a region-based segmentation and knowledge-based classification are integrated. In the segmentation for surface elevation, the LIDAR points are resampled to raster form. A QuickBird multispectral image with is applied in this stage to improve the spectral information. Then, a knowledge-based classification procedure considering spectral, shape, texture, and elevation information is performed to detect the building regions. In the stage of building reconstruction, building blocks are divided and conquered. Once the building regions are detected, we analyze the coplanarity of the LIDAR raw data to shape the roof. Then, we perform TIN-based region growing to generate 3D planes for a building region. The accurate position of walls of the building is determined by the edges extracted from aerial images. Thus the three dimensional building edges can be used for the reconstruction.

A patented method SMS (Rau and Chen, 2003) is then employed to generate building models in the last step. Having the advantages of high reliability and flexibility, the SMS method provides stable reconstruction even when those 3D building lines are broken. The feature of SMS method allows incomplete 3D building lines due to occlusions or weak image features.

2. PREPROCESSING

The data preprocessing consists of two steps, which are interpolation of LIDAR data and space registration.

---

* Corresponding author.

2.1 Interpolation LIDAR Data

The LIDAR data includes ground point data and surface point data. The procedure starts from resampling the two sets of discrete points from LIDAR data into regular grid as DTM and DSM (Briese et al, 2002), respectively. A TIN-based interpolation method is applied to rasterize the LIDAR data (Behan, 2000).

2.2 Space Registration

Space registration is another preprocessing of data fusion. The objective of space registration is to build-up the relationship between LIDAR space and image space. We use ground control points to build the mathematic model for space registration. Hence, the LIDAR data and image data are coregistered in the same georeference system.

3. BUILDING DETECTION

The objective of building detection is to extract the building regions. There are two steps in our scheme: (1) region-based segmentation, and (2) knowledge-based classification. The flow chart of building detection is shown in Figure 1.
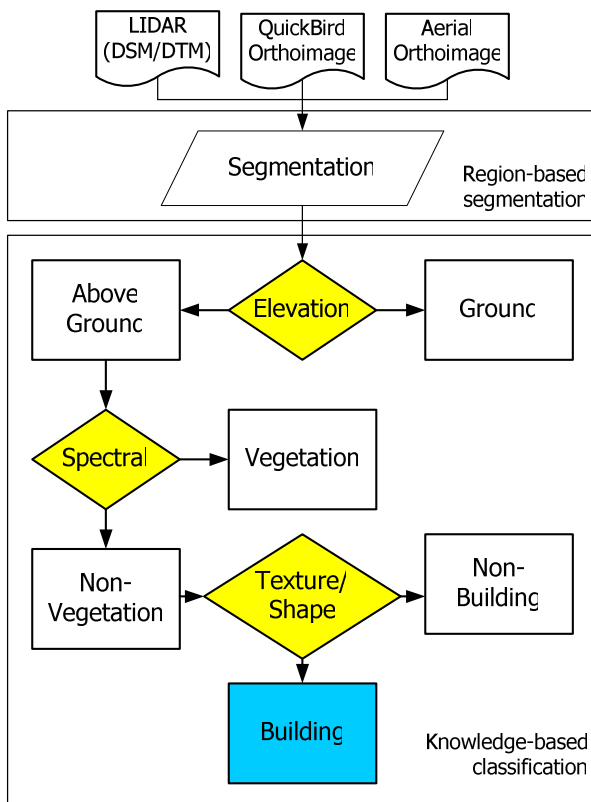

Figure 1. Flow chart of building detection.

3.1 Region-based Segmentation

There are two ways to do the segmentation. The first one is the contour-based segmentation. It performs the segmentation by using edge information. The second one is the region-based segmentation. It uses a region growing technique to merge pixels with similar attribute (Lohmann, 2002). We select the region-based segmentation because its noise tolerance is better than contour-based segmentation. We combine elevation attribute from LIDAR data and radiometric attribute from orthoimages in the segmentation. The pixels with similar height and spectral attribute are merged into a region.

3.2 knowledge-based classification

After segmentation, an object-based classification rather than pixel-based classification is performed. Each separated region after segmentation is a candidate object for classification. A knowledge-based classification considering elevation, spectral, texture, and shape information is performed to detect the building regions (Hofmann, et. al, 2001). The LIDAR data, QuickBird multispectral image and aerial image are integrated in this stage. A number of characteristics of these data are considered to obtain the knowledge for classification. The characteristics are described as follow.

Elevation: Subtract DTM from DSM, we will get the normalized DSM (nDSM), which contains the height information above ground. It represents the objects rising from the ground. Setting an elevation threshold one can separate the object above ground and on the ground. The above ground surface includes building and vegetation that are higher than the elevation threshold.

Spectral: The spectral information comes from QuickBird multispectral images, which contains blue, green, red, and near infrared bands. The near infrared band gives the useful spectral information for vegetation. A well-known Normalized Vegetation Index (NDVI) is used to distinguish vegetation from non-vegetation areas.

Texture: Several papers demonstrated that texture information is useful for building detection (Zhang, 1999). The texture information comes from high spatial resolution aerial images. We use the Grey Level Co-occurrence Matrix (GLCM) for texture analysis. This is a matrix of relative frequencies for pixel values occur in two neighboring processing windows, in which, we use the entropy and homogeneity to compute the co-occurrence probability. The role of texture information is used to separate the building and vegetation when the objects have similar spectral response.

Shape: The shape attribute includes area and length-to-width ratio. The area attribute can be used to filter those small size objects. The length-to-width ratio is suitable to remove the thin objects.

4. BUILDING RECONSTRUCTION

After extracting building region, each individual building region is isolated. Then, we reconstruct the building models for individual building regions. The spatial resolution of aerial image is better than QuickBird multispectral satellite image. Thus, we select aerial image to reconstruct the building models. There are four steps in our schemes: (1) 3D planar patch forming, (2) initial building edge detection, (3) straight line extraction, and (4) split-merge-shape method for building modeling. The flow chart of building reconstruction is shown in Figure 2.
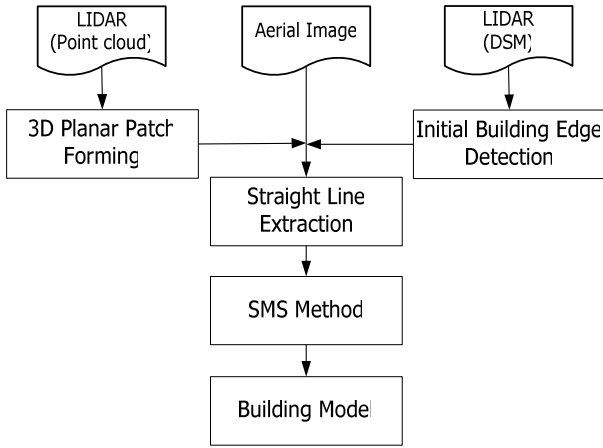
Figure 2. Flow chart of building reconstruction.

4.1 3D Planar Patch Forming

The first stage of building reconstruction is to extract the 3D planar patches from LIDAR data. A TIN-based region growing procedure is presented for 3D planes forming. The coplanarity and adjacency between triangles are considered for TIN-based region growing. Two coplanarity conditions are considered for merging triangles: (1) the angle between normal vectors for neighboring triangles, and (2) the height difference between triangles. When the triangles meet the coplanarity criteria, the triangles will merge together as a same plane. Once the planar segments are extracted, we use least squares regression to determine the coplanarity function of planar segment. Figure 3 is the illustration of formed 3D planar patches.
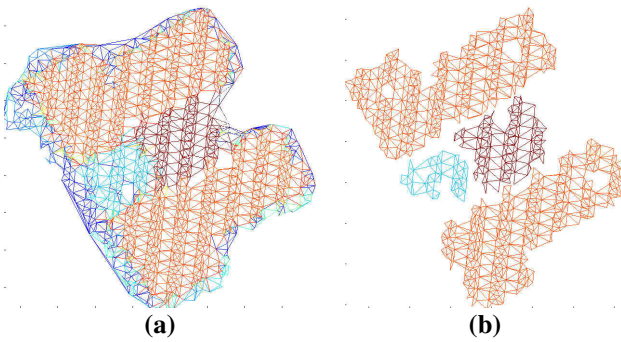

Figure 3. Illustration of 3D planar patching.
    (a) triangular form in building region.
    (b) extracted 3D planar facets.

4.2 Initial Building Edge Detection

After extracted the 3D planes, we detect the initial building edge from raster form LIDAR data. The initial edges in single building region are obtained by a Canny operator (Canny,1986). A 2D line tracking is applied to the edge detection result. Then, we select a length threshold to remove short lines. After removing the short lines, we consider the elevation information of edge to perform the 3D line tracking. Each line is classified to the 3D planar patch as stated. The steps of initial building edge extraction are illustrated in Figure 4.
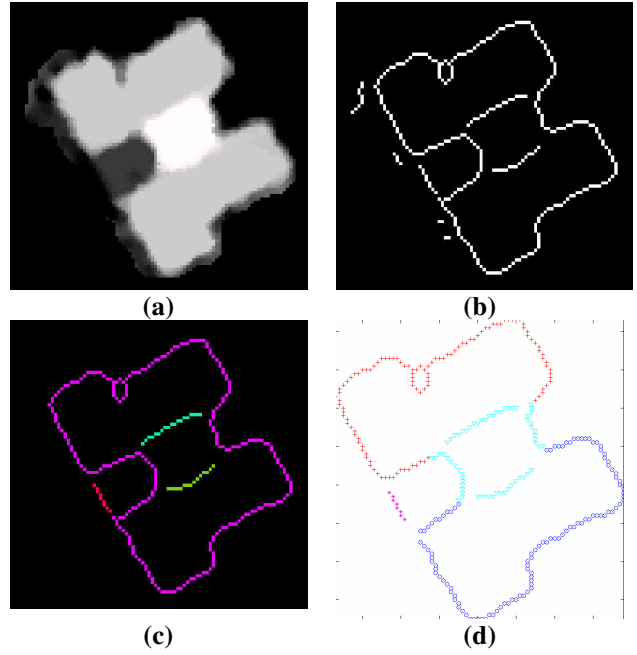

Figure 4. Illustration of initial building edge detection.
    (a) DSM in building region.
    (b) edges detected from Canny operator.
    (c) filtering the short edge by 2D line tracking.
    (d) classified the edges to 3D plane by 3D line tracking.

4.3 Straight Line Extraction

Based on the rough edges, the precise building edges are to be extracted in image space. Through the Hough transform (Hough,1962), straight lines in image space are detected. Given the image coordinates and the height information from 3D planes, we can calculate the 3D edges in the object space by employing exterior orientation parameters. Figure 5 is an example of straight line extraction.
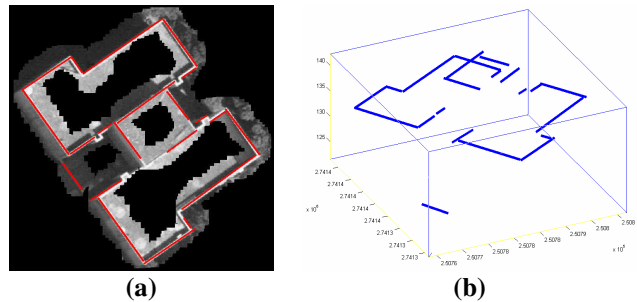

Figure 5. Building boundaries extraction.
    (a) 2D building lines
    (b) 3D building lines

4.4 SMS Method

After the straight line extraction, the accurate 3D edges are combined with the already developed Split-Merge-Shape, SMS method (Rau and Chen, 2003) for building reconstruction. The Split and Merge steps are the two main procedures for topology reconstruction from non-related roof-edges. The Shape step uses the available roof-edge height information to define an appropriate rooftop.

5. EXPERIMENTAL RESULTS

The LIDAR data used in this research covers an area in Hsin-Chu Science-based Industrial Park of north Taiwan. The data was obtained by Leica ALS 40 system. The discrete LIDAR points were classified into ground points and surface points previously. The average density of LIDAR data is about 1.6 pts/m^2. The ground resolution of QuickBird multispectral satellite image and aerial image are 2.8m and 0.1m, respectively. The related parameters are shown in Table 1.

In building detection, the surface points and ground points from LIDAR data are rasterized to DSM and DTM both with a pixel size of 0.5m. The DSM and DTM are shown in Figure 6 and Figure 7. The QuickBird multispectral image and aerial image are rectified into orthoimage by using the LIDAR DSM. The orthoimages of QuickBird and aerial photo are shown in Figure 8 and Figure 9 respectively. The segmentation result is shown in Figure 10. The classification result is shown in Figure 11. A 1/1000 scale topographic map was used to evaluate the classification results. The 1/1000 topographic map is shown in Figure 12. As we compared the classification results and topographic map, most of the building regions are accurately extracted. The small buildings are normally with low elevation and less texture information. Hence, most of the undetected buildings are the small ones. Considering different land covers, the classification accuracy is 94%. On the other hand, if we only considered buildings, the detection rate is 81%. The accuracy performance is demonstrated in Table 2.

Table 1. Related information of test images

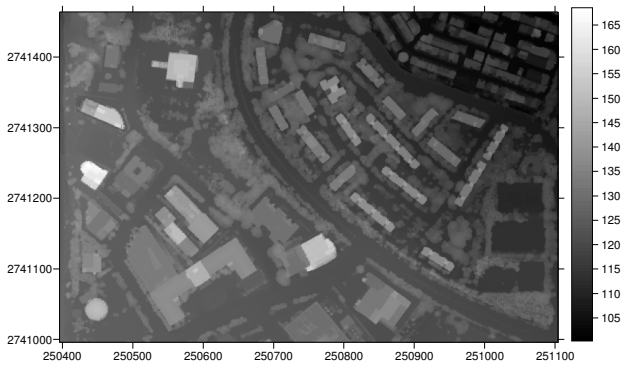|	LIDAR	Optical Images	
	Leica ALS40	Aerial Image	QuickBird Image
Acquire Date	2002.04	2002.03.20	2002.10.17
Resolution	0.8m/point	0.1m/pixel	2.8m/pixel
Data	1.Surface points 2.Ground points	color image	multispectral image

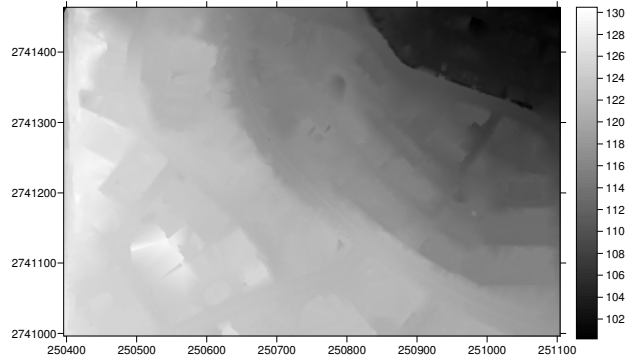

Figure 6. Digital surface model

Figure 7. Digital terrain model

Figure 8. Aerial image
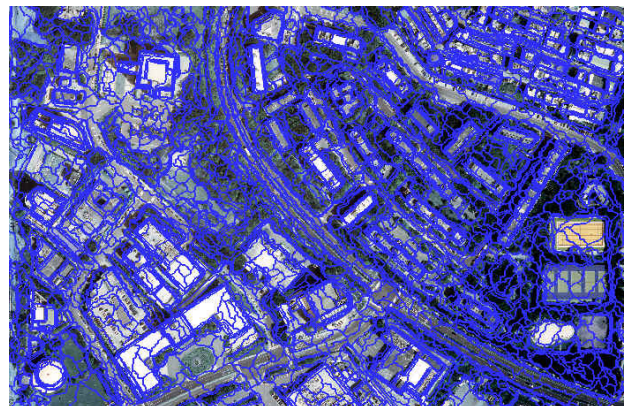

Figure 9. QuickBird multispectral image
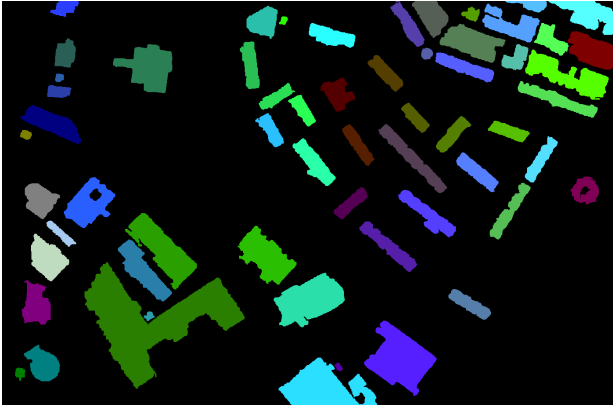

Figure 10. Result of segmentation
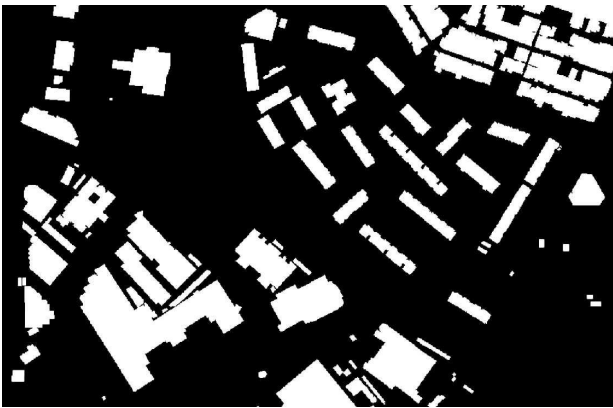
Figure 11. Result of building detection

Figure 12. Building region from 2D topographic map

Table 2. Accuracy assessment for building detection

		Classified Data		
	Unit: pixel	Building	Non Building	Total
Reference Data	Building	a=259685	b=58176	e=317861
	Non Building	c=17565	d=954895	f=972460
	Total	g=277250	h=1013071	i=1290321
	Diagonal Total			1214580
	Producer	a/e=81%	d/f=98%	89.5%
	User	a/g=93%	d/h=94%	93.5%
	Overall (a+d)/i	-	-	94%

For each building region, the 3D planes are extracted by TIN-based region growing. Meanwhile, initial building edges are approximately detected in the DSM. The edges are then projected into aerial image to mark the working area for straight line detection. Through the Hough transform straight line extraction, the precise straight lines which combine the 3D planes can be projected into object space. After combining the 3D lines with SMS method, the building model can be reconstructed. Comparing the coordinates roof corners in the reconstructed models with the corners measured from stereo pairs, the root mean square errors are 0.45m, 0.56m, 0.70m in the X, Y, Z directions, respectively. The results of building models are shown in Figure 13.
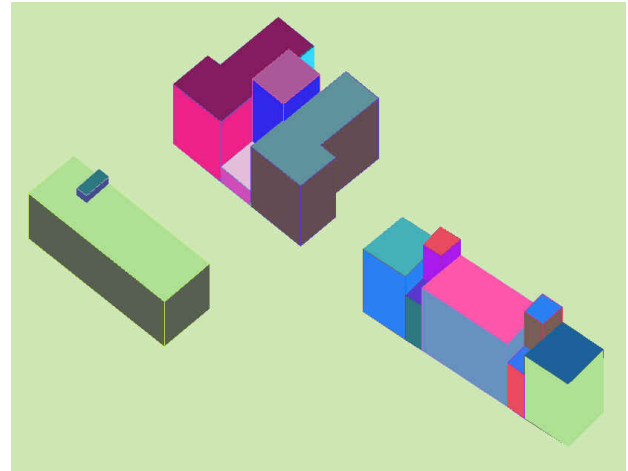

Figure 13. 3D view of generated building model

6. CONCLUSIONS

In this investigation, we have presented a scheme for the extraction of building regions and building modeling by performing fusion of LIDAR data and optical imagery. The results from the test show the potential of the automatic method for building reconstruction. More than 81% buildings region are correctly detected by our approach. The building models generated by the proposed method have the merits of high horizontal accuracy from aerial images and high vertical accuracy from LIDAR data. Comparing the models reconstructed by the proposed method with the reference data from aerial stereo pairs, we achieved sub-meter accuracy. However, in this investigation, we only consider flat roof buildings. The improvements of the scheme for treating more complex buildings are the major works in the future.

REFERENCES

Behan, A., 2000, On the matching accuracy rasterised scanning laser altimeter data. IAPRS, Vol. XXXIII, Part B2, pp.75-82.

Briese, C., Pfeifer, N., and Dorninger, P., 2000, Application of the Robust Interpolation for DTM Determination. IAPRS, vol. XXXIII,pp.55-61.

Canny, J., 1986, A computational approach to edge detection, IEEE Transactions on Pattern Analysis and Machine Intelligence, Vol. PAMI-8, No. 6, pp. 679-698.

Guo, T., 2003, 3D city modeling using high-resolution satellite image and airborne laser scanning data. Doctoral dissertation, Department of Civil Engineering, University of Tokyo, Tokyo.

Hofmann, A.D., Mass, H., Streilein, A., 2002, Knowledge-based building detection based on laser scanner data and topographic map information, IAPRS, Vol.34, Part 3A+B, pp.163-169.

Hough, P.V.C. 1962, Methods and means for recognising comples patterns, U.S. patent No. 306954

Lohmann, P., 2002, Segmentation and filtering of laser scanner digital surface models, IAPRS, Vol. XXXIV, Part 2,, Xi'an,20-23, Aug, 2002, pp311-316

Nakagawa, M., Shibasaki, R., and Kagawa, Y., 2002, Fusion Stereo Linear CCD Image and Laser Range Data for Building 3D Urban Model, IAPRS, Vol.34, Part 4, pp. 200-211.

Rau, J. Y., and Chen, L. C., 2003, Robust reconstruction of building models from three-dimensional line segments, Photogrammetric Engineering and Remote Sensing, Vol. 69, pp.181-188.

Rottensteiner, F., and Jansa, J., 2002, Automatic Extraction of Building from LIDAR Data and Aerial Images, IAPRS, Vol.34, Part 4, pp. 295-301.

Vosselman, G., 2002, Fusion of laser scanning data, maps and aerial photographs for building reconstruction, International Geoscience and Remote Sensing Symposium, 2002, 24-28 June, Toronto,Canada, on CD-ROM.

Zhang, Y., 1999, Optimisation of building detection in satellite images by combining multispectral classification and texture filtering, ISPRS Journal of Photogrammetry & Remote Sensing, Vol.54, pp.50-60.